Velocity dependence of outgoing neutral fractions for H(1*s*) and H^+ beams impinging on Al(111) at grazing incidence

H. Jouin[1,*] and F. A. Gutierrez[2]

[1]*CELIA (UMR 5107 Université Bordeaux 1-CNRS-CEA), Université Bordeaux 1, 351 Cours de la Libération, F-33405 Talence Cedex, France*

[2]*Departamento de Física, Universidad de Concepción Casilla 160-C, Concepción, Chile*

(Received 7 June 2011; published 25 July 2011)

Neutral fractions of scattered ground-state hydrogen atoms after grazing incidence collisions of both H(1*s*) and H^+ projectiles with an Al(111) surface have been computed within the impact velocity range $0.1 \leqslant v \leqslant 2.0$ a.u. by means of the ETISC1D code. Comparison between the results related to the H(1*s*) beam with those obtained for H^+ projectiles—which we found in earlier work to be in good agreement with experimental data—shows that in the velocity range $0.3 \leqslant v \leqslant 1.3$ a.u. neutral fractions keep the memory of the initial state, whereas in the extreme ranges of low velocities ($v \lesssim 0.3$ a.u.) and high velocities ($v \gtrsim 1.3$ a.u.), the outgoing charge fractions do not depend on the charge state of the initial beam. In order to analyze qualitatively these findings, rate-equations calculations as well as a simplified analytical model have been also implemented. Due to the lack of experimental data for impinging H(1*s*), the present results represent important theoretical predictions which might stimulate further experimental works.

DOI: 10.1103/PhysRevA.84.014901 PACS number(s): 79.20.Rf, 73.20.Mf, 79.20.Fv

In two recent theoretical works [1,2] we have analyzed in some detail the interaction between protons and metal surfaces at grazing incidences. In [1] we obtained outgoing neutral fractions (NF) corresponding to H^+ impinging on Al(111) in the velocity range $0.1 \leqslant v \leqslant 2$ a.u., while in [2] we have computed angular distributions (AD) of scattered ground-state hydrogen atoms for several impact energies. For both NF and AD we have obtained a good agreement with available experimental data [3,4]. The present work deals with a comparison between NF corresponding to H^+ and H^0 impinging on Al(111) at small incidence angles in a wide range of impact velocities. As concluded in pioneering works [5–7] in the field of ion-surface collisions, NF corresponding to both incident charge states should be identical at all velocities since the so called "memory term" [5–7] vanishes for realistic ion-surface encounters in such a way that the atomic species lose the memory of their initial state during their travel in the surface's vicinity. We will show in what follows that it is the case in the extreme ranges of low velocities ($v \lesssim 0.3$ a.u.) and high velocities ($v \gtrsim 1.3$ a.u.), whereas in the intermediate range NF corresponding to both incident projectiles present noticeable differences which are basically due to velocity changes experienced by the particles when electronic transitions take place.

The main part of the present calculations have been performed by means of a numerical approach implemented within the ETISC1D code constructed for grazing-incidence particle-surface collisions [8]. As this method has been presented in detail in previous works [1,2,8], it will be briefly summarized in what follows. Particle's parallel velocity ($v_\parallel$) is kept constant while the perpendicular motion of the ionic (or atomic) species is obtained by integration of Hamilton-Jacobi equations in which the scattering potential is changed when the charge state of the species varies due to electron charge transfer processes. These latters are taken into account through their respectives transition rates complemented by a Monte Carlo type procedure that allows us to simulate the possibility of an electronic transition during a time step corresponding to the integration of Hamilton-Jacobi equations. This time step must be chosen small enough to reach an accurate numerical integration, but also large enough to allow the projectile to "become aware" of its new interaction with the surface, before its state is analyzed within the next time step. In that way, one obtains the position, the momentum, and the charge state of each particle of the beam at every time. The purely repulsive potential felt by hydrogen atoms, at a distance z from the first atomic layer, $U_0(z)$ is obtained by averaging over the first atomic plane individual interatomic potentials represented by a Ziegler-Biersack-Littmark screening function [9]. The potential $U_+(z, v_\parallel)$ experienced by protons is described as the sum of the planar potential $U_0(z)$ plus the attractive dynamical image potential $U_I(z, v_\parallel)$ which we describe, for practical reasons, through a fit [1] of the velocity-dependent potential calculated by García de Abajo and Echenique [10]. For the transition rates toward the ground state of hydrogen (the weak population of excited states is not accounted for) we have used here the result of Nordlander and Tully [11] for the static resonant capture transition rate and the one of Hentschke *et al.* [12] for the static two-electron Auger capture rate. To obtain velocity-dependent transition rates from the static ones for both resonant [resonant capture (RC) and resonant loss (RL)] and Auger transitions [Auger capture (AC) and Auger loss (AL)] we use the approximate "kinematic factor" approach of Mišković and Janev [13]. We also take into account the surface-plasmon-assisted electron-capture process [pure surface plasmon (PSP)] through the velocity dependent rates reported in [1,14].

In Fig. 1 we display neutral fractions as functions of the impact velocity (for a grazing angle of incidence of 0.56°) obtained with the ETISC1D code for ingoing H^+ and H(1*s*) projectiles. In the case of incident protons, we have shown in Ref. [1] that our results are in pretty good agreement with experimental measurements. Unfortunately, to our knowledge,

*jouin@celia.u-bordeaux1.fr

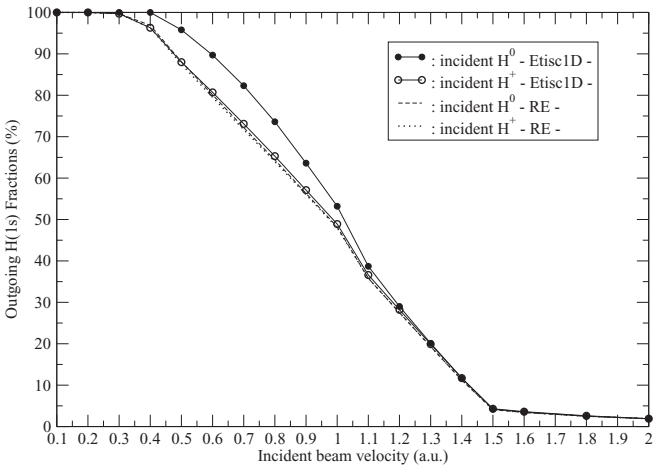

FIG. 1. Outgoing H(1s) fractions (%) as functions of the velocity for an angle of incidence of 0.56°. Full line with filled (empty) circles: neutral fractions obtained with the ETISC1D code (see text) for an H^0 (H^+) incident beam. Dashed (dotted) line: neutral fractions calculated by means of the RE method (see text) for an H^0 (H^+) impinging beam.

experimental data for incoming neutrals have not been reported so far in the literature.

One can see from Fig. 1 that outgoing neutral fractions corresponding to both incident charge states are identical at low impact velocities ($v \leqslant 0.3$ a.u.) and also in the high velocity range ($v \geqslant 1.3$ a.u.). At intermediate velocities ($0.3 \leqslant v \leqslant 1.3$), outgoing neutral fractions corresponding to impinging neutrals present higher values than those related to incoming protons (up to 10% around $v = 0.6$). The 100% neutral fractions for both incident beams at low velocities can be easily understood remembering from Refs. [1,2] that the total capture rate $[\Gamma_C(z,v_\parallel) = \Gamma_{RC}(z,v_\parallel) + \Gamma_{AC}(z,v_\parallel) + \Gamma_{PSP}(z,v_\parallel)]$ is various orders of magnitude greater than the total loss rate $[\Gamma_L(z,v_\parallel) = \Gamma_{RL}(z,v_\parallel) + \Gamma_{AL}(z,v_\parallel)]$ in this velocity range. In that way, incoming protons capture easily an electron and the corresponding beam reach rapidly the total neutralization up to $v \simeq 0.3$ a.u. Conversely, the atoms of the neutral incoming beam cannot lose their electrons, remaining in their initial state up to $v \simeq 0.4$ a.u.

Similar calculations using the static resonant rates computed in Refs. [15,17] have also been performed (results not shown for the sake of conciseness). Thus, we have checked that for impinging H^0, outgoing neutral fractions obtained by means of these various resonant rates present weak variations analogous to those already reported in Ref. [1] for ingoing H^+. A detailed analysis of this somewhat surprising result—if one remembers the noticeable differences between the static resonant rates reported in [11,15–17]—can be found in Ref. [1].

To gain more insight on the behaviors shown in Fig. 1 and particularly on the high velocity regime, we have also calculated outgoing neutral fractions by means of the rate equations (RE) approach which was used in the pioneering works [5–7]. In the present case, this latter scheme reduces to the following set of first-order differential equations with the initial conditions $P_g(t \to -\infty, v_\parallel) = \beta_i$ and $P_+(t \to -\infty, v_\parallel) = 1 - \beta_i$ (with β_i the fraction of neutral atoms in the initial beam, $0 \leqslant \beta_i \leqslant 1$):

$$dP_g(t,v_\parallel)/dt = \Gamma_C(t,v_\parallel)\,P_+(t,v_\parallel) - \Gamma_L(t,v_\parallel)\,P_g(t,v_\parallel), \tag{1a}$$

$$dP_+(t,v_\parallel)/dt = -\Gamma_C(t,v_\parallel)\,P_+(t,v_\parallel) + \Gamma_L(t,v_\parallel)\,P_g(t,v_\parallel), \tag{1b}$$

where P_g and P_+ are the neutral fraction and the proton's population, respectively. In order to integrate this set of equations, it is necessary to use the transformation $dt = dz/v_\perp^{(i)}$, since all the transition rates are calculated [1,11,12,14–18], as functions of the particle-surface distance (and not as functions of time). This transformation leads to the following set of differential equations which are integrated by means of a Runge-Kutta algorithm:

$$dP_g(z,v_\parallel)/dz = [\Gamma_C(z,v_\parallel)\,P_+(z,v_\parallel) - \Gamma_L(z,v_\parallel)\,P_g(z,v_\parallel)]\,/\,v_\perp^{(i)}, \tag{2a}$$

$$dP_+(z,v_\parallel)/dz = [-\Gamma_C(z,v_\parallel)\,P_+(z,v_\parallel) + \Gamma_L(z,v_\parallel)\,P_g(z,v_\parallel)]\,/\,v_\perp^{(i)}, \tag{2b}$$

The above transformation from time to space requires obviously the introduction of a normal velocity $v_\perp^{(i)}$ which turns to be the main drawback of the RE approach with respect to the one implemented in the ETISC1D simulation since the former approach cannot account for the velocity change of a particle whose charge state varies. Hence, for the RE method the definition of $v_\perp^{(i)}$ is somewhat arbitrary and it is taken here as the normal velocity of the incident beam at $z_{max.}$, when it penetrates the simulation box in which the transition rates present nonnegligible values (here the simulation box ranges from the position of the first atomic layer at $z = 0$ to $z_{max} = 13.3$ a.u.). Thus, in the case of impinging neutrals, $v_\perp^{(0)}$ is slightly smaller (at low v) than the asymptotic perpendicular velocity of the beam $[v_\perp^{(\infty)} = v\,\sin(\Phi_{in})$ where Φ_{in} is the angle of incidence] since neutrals are weakly slowed down by the repulsive potential $U_0(z)$ at large distances; however for $v \gtrsim 1$ a.u., both velocities are identical. Conversely, protons are accelerated at large distances by the Coulombic tail of the image potential $U_I(z,v_\parallel)$ in such a way that $v_\perp^{(+)}$ is much greater than $v_\perp^{(\infty)}$ at low velocities (a factor of 5 for $v = 0.1$) although this difference weakens for increasing velocities. In the high velocity range ($v \geqslant 1.3$), $v_\perp^{(+)}$ is very close to $v_\perp^{(0)}$ with relative differences smaller than 8%.

Neutral fractions obtained from the RE method for H^0 and H^+ incident beams are also reported in Fig. 1 where one can see that both results are almost identical in the whole velocity range. Furthermore, these results are also very close to the neutral fraction computed by means of ETISC1D for impinging protons. This means that ETISC1D and RE approaches provides the same outgoing neutral fractions for impinging H^+, while for incoming neutrals NF obtained by both methods are the same only at low and high velocities. In the intermediate velocity range, NF obtained with ETISC1D for incoming H^0 are greater than those calculated by means of the RE method with a maximum absolute difference of 10% around $v = 0.7$. The inaccurate result provided by the RE approach for incident

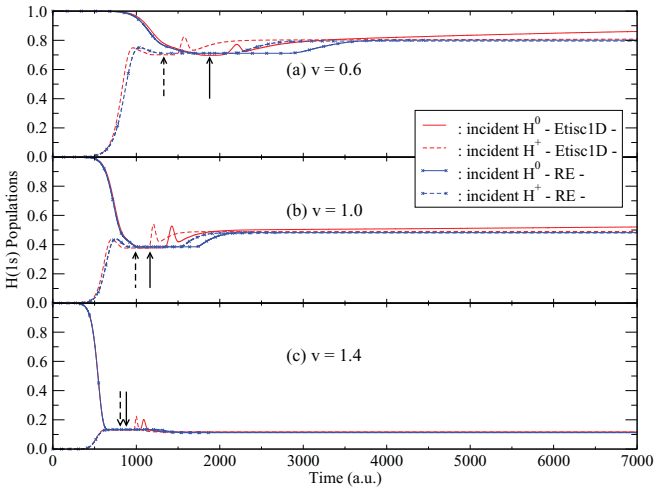

FIG. 2. (Color online) H(1s) populations as functions of time for (a) $v = 0.6$, (b) $v = 1.0$, and (c) $v = 1.4$. Full (red) line: ETISC1D calculation for an H^0 incident beam. Dashed (red) line: ETISC1D calculation for an H^+ incident beam. Full (blue) line with $\times$: RE calculation for an H^0 incident beam. Dashed (blue) line with $\times$: RE calculation for an H^+ incident beam. Vertical arrows indicate the location of turning points in ETISC1D calculations: full line arrows for impinging H^0 and dashed line arrows for ingoing H^+.

H^0 in the intermediate range is related to the fact that velocity variations cannot be taken into account in the frame of this approach.

A further discussion of the above results can be done by means of the H(1s) populations as functions of time displayed in Fig. 2 for three representatives velocities ($v = 0.6$, $v = 1.0$, and $v = 1.4$). First, it must be mentioned that in the RE approach, populations are obtained as functions of the spatial coordinate z, in such a way that we use the transformation $t = z/v_\perp^{(i)}$ to represent RE populations as functions of time in Fig. 2. One can see in Figs. 2(a)–2(c) that the RE method allows us to reproduce quite well the earlier stage of variation (depopulation for incoming H^0 or population for ingoing protons) with respect to the reference ETISC1D results. Weak differences between both methods detected at low velocities get reduced with increasing velocity. This means that the velocities used in RE calculations are approximately the correct ones for this first step. However, in the outgoing path of the collision the RE result departs noticeably from the ETISC1D one for impinging neutrals for the two lowest velocities. The ETISC1D calculation shows a very slow repopulation of the fraction of the incident beam which has lost his electron. This behavior that is not present in the RE results yields the NF reported in Fig. 1 for impinging H^0 in the velocity range $0.3 \leqslant v \leqslant 1.3$ and can be explained as follows. When a ground-state hydrogen is ionized in the ingoing path of the collision, the normal velocity of the created proton can increase drastically for low v with respect to the one of the incoming atom (up to an order of magnitude for $v = 0.6$, which reduces to a factor of 2 for $v = 1.0$ and to 50% at $v = 1.4$). This high normal velocity gained by protons at low v slows down the dynamics of the later recapture process (in spite of the important values of capture rates at low v) and also explains the fail of the RE method in reproducing this dynamics since this strong velocity change is not accounted for in that approach. This slow dynamics of the recapture process disappears for increasing velocities since, as stated before, the velocity changes weakens for high velocities with the other consequence that the RE method works better in the high velocity range leading to the same NF as ETISC1D. For impinging H^+, it is clear from Figs. 1 and 2(a)–2(c) that the RE approach provides almost the same NF as ETISC1D in the whole range of impact velocities considered here. This is basically due to the fact that the depopulation process that follows the initial population step is weak for all velocities [see Figs. 2(a)–2(c)] in such a way that the velocity changes (which can be obviously as strong as in the case of ingoing neutrals) affect only a small fraction of the beam.

In Fig. 2(c), which is representative of the high velocity regime ($v \geqslant 1.3$), one can observe that the time evolution of populations obtained by both methods is very similar for the two kinds of projectiles. Moreover, the H(1s) populations corresponding to incident H^0 and to incident H^+ converge very rapidly to the same value at the end of the initial path (close to the image plane) and furthermore, this value does not vary significantly as time goes on. These behaviors may be understood at least qualitatively remembering first that at high velocities the normal velocities of both projectiles are almost the same and that velocity changes due to the scattering potentials are relatively weak. Moreover in that velocity range, loss rates are several orders of magnitude greater than the capture ones so that the loss mechanism is important for ingoing neutrals while the capture process is weak for incoming protons. In that way, it is not so surprising that the populations corresponding to both incident charge state merge at some instant of the dynamics.

A deeper qualitative understanding of the above features can be obtained by direct analytical integration of the differential equations system of Eqs. (2) with the help of the approximated representations for both the total capture and total loss rates:

$$\Gamma_C(z \geqslant d_{\rm im}, v_\parallel) = \Gamma_{C_M}(v_\parallel)\, \exp[-\gamma(v_\parallel)(z - d_{\rm im})], \quad (3a)$$

$$\Gamma_L(z \geqslant d_{\rm im}, v_\parallel) = \Gamma_{L_M}(v_\parallel)\, \exp[-\gamma(v_\parallel)(z - d_{\rm im})], \quad (3b)$$

with also $\Gamma_C(z < d_{\rm im}, v_\parallel) = \Gamma_L(z < d_{\rm im}, v_\parallel) = 0$ $\{d_{\rm im} = 3.2955$ for Al(111) [19]$\}$. With this description, that approximately represents the rates as we shall see below, we obtain the following expressions for the neutral fractions in the incoming and in the outgoing pathways $P_g^I(z : +\infty \longrightarrow d_{\rm im})$ and $P_g^O(z : d_{\rm im} \longrightarrow +\infty)$, respectively,

$$P_g^I(z, v_\parallel) = [\beta_i - \mathcal{R}_{C_M}(v_\parallel)]\, \exp\{-\lambda(v_\parallel) \times \exp[-\gamma(v_\parallel)(z - d_{\rm im})]\} + \mathcal{R}_{C_M}(v_\parallel), \quad (4a)$$

$$P_g^O(z, v_\parallel) = \mathcal{M}(v_\parallel)\, \exp\{+\lambda(v_\parallel) \exp[-\gamma(v_\parallel)(z - d_{\rm im})]\} + \mathcal{R}_{C_M}(v_\parallel), \quad (4b)$$

where $\mathcal{M}(v_\parallel) = [\beta_i - \mathcal{R}_{C_M}(v_\parallel)]\, \exp[-2\,\lambda(v_\parallel)]$, a value which results from the matching condition at $z = d_{\rm im}$: $P_g^O(z = d_{\rm im}, v_\parallel) = P_g^I(z = d_{\rm im}, v_\parallel)$ and

$$\lambda(v_\parallel) = [\,\Gamma_{C_M}(v_\parallel) + \Gamma_{L_M}(v_\parallel)]/[v_\perp^{(i)}\, \gamma(v_\parallel)], \quad (5a)$$

$$\mathcal{R}_{C_M}(v_\parallel) = \Gamma_{C_M}(v_\parallel)/[\,\Gamma_{C_M}(v_\parallel) + \Gamma_{L_M}(v_\parallel)], \quad (5b)$$

From Eqs. (4), it appears clearly that strictly speaking the final NF [i.e., $P_g^O(z \longrightarrow +\infty, v_\parallel)$] still depends upon the initial condition β_i {through the factor $\mathcal{M}(v_\parallel)$ which was called "memory term" in [5–7]} or in other words on the charge state of the incoming beam. However, if the factor $\lambda(v_\parallel)$ is strong enough to allow the term $\exp\{-\lambda(v_\parallel)\exp[-\gamma(v_\parallel)(z - d_{\rm im})]\}$ of Eq. (4a) to become very small [with respect to the $\mathcal{R}_{C_M}(v_\parallel)$ value] at some point z^* of the ingoing path, then $P_g^I(z = d_{\rm im}, v_\parallel) \simeq \mathcal{R}_{C_M}(v_\parallel)$ with the consequence that $\mathcal{M}(v_\parallel) \simeq 0$ and finally $P_g^O(z, v_\parallel) \simeq \mathcal{R}_{C_M}(v_\parallel)$ (for all z values in the exit pathway) which means that when neutral populations corresponding to the two incident beams have reached at z^* the saturation value $\mathcal{R}_{C_M}(v_\parallel)$, these populations do not evolve anymore. This is exactly what happens in the high velocity range ($v \geqslant 1.3$) as it can be seen in Fig. 2(c).

As an illustration, in Fig. 3, we compare for $v = 1.4$ the populations obtained from the analytical expressions given in Eqs. (4) with those obtained by numerical integration of RE equations of Eqs. (2) for both incident neutral atoms and protons. The analytical solution is close to the numerical one with some minor differences which are obviously due to the approximate description of the rates by means of Eqs. (3) needed for the analytical resolution. These approximate rates as well as the sum of capture rates and the sum of loss rates for $v_\parallel = 1.4$ (used in RE and ETISC1D calculations) are displayed in the inset of Fig. 3. It is clear that both analytical and numerical results indicate that the populations corresponding to impinging H^0 and H^+ species merge around 1 a.u. in front of the image plane in the incoming pathway and that there is no further variation between these populations leading to the result of Fig. 1 at high velocities.

Calculations of neutral fractions of scattered ground-state hydrogen atoms after grazing incidence collisions of both H(1s) and H^+ projectiles with an Al(111) surface within the impact velocity range $0.1 \leqslant v \leqslant 2.0$ a.u., allow us to show that in the extreme ranges of low velocities ($v \lesssim 0.3$ a.u.) and high velocities ($v \gtrsim 1.3$ a.u.), the outgoing charge fractions do not depend on the charge state of the initial beam. In these velocity ranges, the ion-surface collision dynamics may be treated through a rate-equations approach (and further analytical models) as it has been done in pioneering works in which it was shown that the final fractions do not depend on the initial state. Nevertheless, in the intermediate velocity range $0.3 \leqslant v \leqslant 1.3$, our results show that the NF keep the memory of the initial charge state due to velocity changes of the particles which can not be accounted for by a RE method. We hope that the present results will stimulate further NF measurements for ingoing hydrogen atoms at grazing incidence.

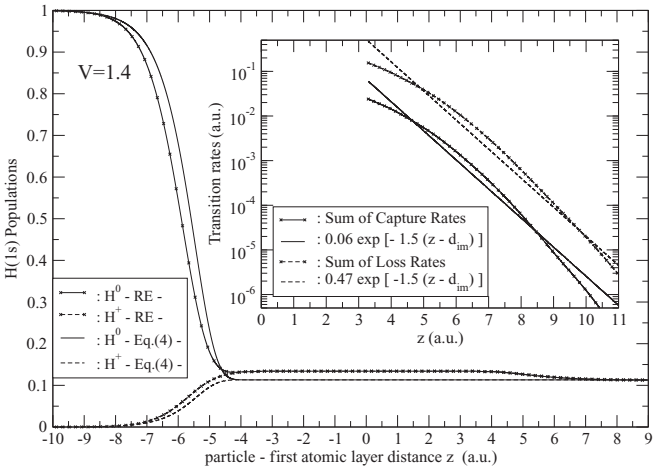

FIG. 3. H(1s) populations as functions of the particle, first layer distance z for $v = 1.4$. Full line with $\times$: RE calculation for an H^0 incident beam. Full line: analytical solution given in Eqs. (4) for an H^0 incident beam ($v_\perp^{(0)} = 0.0137$). Dashed line with $\times$: RE calculation for an H^+ incident beam. Dashed line: analytical solution given in Eqs. (4) for an H^+ incident beam ($v_\perp^{(+)} = 0.0146$). Inset: Transition rates as functions of z for $v_\parallel = 1.4$. Full line with $\times$: Sum of capture rates (RC + AC + PSP). Full line: description of the previous rate by means of Eq. (3a) with $\Gamma_{C_M}(1.4) = 0.06$ and $\gamma(1.4) = 1.5$. Dashed line with $\times$: Sum of loss rates (RL + AL). Dashed line: description of the previous rate by means of Eq. (3b) with $\Gamma_{C_M}(1.4) = 0.47$ (and $\gamma(1.4) = 1.5$).

The collaboration between the "Sources X, Plasmas and Ions" Group at CELIA (Bordeaux, France) and the Atomic Collision Group at the Universidad de Concepción, Chile has been partially supported by the projects FONDECYT (regular) 1061003 and FONDECYT (Colaboracion Internacional) 7080171 and 7090091.

[1] H. Jouin and F. A. Gutierrez, Phys. Rev. A **80**, 042901 (2009).
[2] F. A. Gutierrez and H. Jouin, Phys. Rev. A **81**, 062901 (2010).
[3] H. Winter, Phys. Rep. **367**, 387 (2002).
[4] H. Winter and M. Sommer, Phys. Lett. A **168**, 409 (1992).
[5] E. G. Overbosch *et al.*, Surf. Sci. **92**, 310 (1980).
[6] R. Brako and D. M. Newns, Surf. Sci. **108**, 253 (1981).
[7] J. Los and J. J. C. Geerlings, Phys. Rep. **190**, 133 (1990).
[8] S. Jequier *et al.*, Surf. Sci. **570**, 189 (2004).
[9] J. P. Ziegler, J. P. Biersack, and U. Littmark, *The Stopping and Range of Ions in Solids* (Pergamon, New York, 1985).
[10] F. J. Garcia de Abajo and P. M. Echenique, Phys. Rev. B **48**, 13399 (1993); F. J. García de Abajo, Ph. D thesis, The University of the Basque Country, San Sebastián, 1993.
[11] P. Nordlander and J. C. Tully, Phys. Rev. B **42**, 5564 (1990).
[12] R. Hentschke *et al.*, Surf. Sci. **173**, 565 (1986).
[13] Z. L. Mišković and R. K. Janev, Surf. Sci. **221**, 317 (1989).
[14] R. Sandoval, F. A. Gutierrez, and H. Jouin, Nucl. Instrum. Methods Phys. Res. Sect. B **258**, 44 (2007).
[15] A. G. Borisov, D. Teillet-Billy, and J. P. Gauyacq, Nucl. Instrum. Methods Phys. Res. Sect. B **78**, 49 (1993).
[16] S. A. Deutscher, X. Yang, and J. Burgdörfer, Phys. Rev. A **55**, 466 (1997).
[17] P. Kurpick, U. Thumm, and U. Wille, Phys. Rev. A **56**, 543 (1997).
[18] F. Martín and M. F. Politis, Surf. Sci. **356**, 247 (1996).
[19] P. A. Serena, J. M. Soler, and N. Garcia, Europhys. Lett. **8**, 185 (1989).